Segmentation of Myocardium Using Velocity Field Constrained Front Propagation

Alexandra L.N. Wong, Huafeng Liu, and Pengcheng Shi*
Hong Kong University of Science and Technology
Department of Electrical and Electronic Engineering
Clear Water Bay, Kowloon, Hong Kong
{alex,eeliuhf,eeship*}@ust.hk

Abstract

We present a velocity-constrained front propagation approach for myocardium segmentation from magnetic resonance intensity image (MRI) and its matching phase contrast velocity (PCV) images. Our curve evolution criterion is dependent on the prior probability distribution of the myocardial boundary and the conditional boundary probability distribution, which is constructed from the MRI intensity gradient, the PCV magnitude, and the local phase coherence of the PCV direction. A two-step boundary finding strategy is employed to facilitate the computation. For the first image frame, a gradient-only fast marching/level set step is used to approach the boundary, and a narrowband is formed around the curve. The initial boundary is then refined using the full information from priors and all three image sources. For the other frames, the resulting contours from the previous frames are used as the initialization contours, and only refinement step is needed. Experiment results from canine MRI sequence are presented, and are compared to results from gradient-only segmentation.

1. Introduction

Acute and chronic myocardial ischemia can be identified and localized through the detection of morphological and kinematics abnormalities of the left ventricle. Thus, accurate and robust measurements of the cardiac geometry and kinematics from image sequence are of important clinical significance, in addition to their technical merits in computer vision research. As the first step, one often needs to isolate the myocardium throughout the cardiac cycle from the background information before further processing.

There have been many segmentation efforts with possible applications to cardiac image analysis [3]. In particular, level set method for curve evolution analysis, and the associated narrow band and fast marching strategies, has gained a lot of popularity recently, given the formulation's invariance to topological changes and its trivial initialization [9]. The convergence of this formulation for shape modeling is usually achieved using gradient-based image features.

It has been recognized that it is often difficult to achieve good segmentation results solely from gradient information. Integration of multiple data and model constraints would often provide more robust result. In [10], image gradient and active contour features are combined with statistical region growing information with a generalized Bayes/MDL criterion. A game theory based framework is adopted to achieve a balanced outcome between region-based segmentation and gradient-based boundary finding in [1].

More directly related to our work, directional information is used as *a priori* knowledge, along with blood flow speed maps, within a Markov random field model for vascular structures segmentation from magnetic resonance angiograms [2]. A level set method is also proposed for myocardium segmentation using coupled front propagation of two curves, one each for endocardium and epicardium [6]. This latter approach unifies region and boundary information with the geodesic active region model, and maintains a constant distance constraint between the coupled contours.

We are presenting a constrained front propagation framework for myocardium segmentation from MR phase contrast images. Three image-driven constraints, the gradient of the MR intensity images, the distribution of the MR phase contrast velocity magnitude, and the local coherence map of the velocity direction, are used as statistical measures to guide the curve evolution. The conditional boundary probability is constructed from these three elements, and a rough-to-fine two-step process is adopted for localizing the myocardial boundaries. We have applied our method to canine cardiac image sequence, and achieved visually more appropriate results than using image gradient alone.

2. Methodology

Our segmentation framework takes advantages of the specific information provided by the MR phase contrast velocity images. First, the gradient information of the MR intensity image is used to drive the evolving curve quickly approaching the boundary, based upon fast marching and level set schemes. Secondly, with the result of the first step, a narrow-band is constructed around the initial curve. Within this narrow-band, the curve is refined with an overall statistical constraint built from any prior knowledge of the boundary location distribution, the image gradient, the phase velocity direction, and the velocity magnitude.

2.1. MR Phase Contrast Images

MR phase contrast velocity imaging relies on the fact that a uniform motion of tissue in the presence of a magnetic field gradient produces a change in the MR signal phase, φ, that is proportional to its velocity [7]:

$$\varphi = v\gamma M_1 = v\gamma \int_0^{TE} t\, G(t)\; dt \qquad (1)$$

where $G(t)$ is the magnetic gradient strength (the gradient waveform), v is the tissue velocity, M_1 is the first moment of the gradient waveform, TE is the echo delay time, and γ is the gyro-magnetic ratio. The gradient waveform can be modified to alter the first moment (motion sensitivity) while maintaining the same image localization characteristics. Images acquired with this altered waveform will have a different phase shift due to motion, and the velocity in a particular spatial direction can be estimated by measuring the difference in phase shift between two acquisitions with different first gradient moments. Hence, instantaneous velocity maps encoded for motion in all three spatial dimensions may easily be obtained at multiple time instances throughout the cardiac cycle using a phase contrast cine-MR imaging sequence. Figure 1 shows an example of the matched 2D phase contrast images of a canine mid-ventricle slice, and the plot of the velocity vectors over the MR intensity image. Since the velocity maps could be quite noisy due to spatial averaging of the region-of-interest (ROI) as well as the blood turbulence, especially at the myocardial boundaries, filtering of the velocity data using techniques such as tensor diffusion may be required to get more robust velocity information [5].

It is important to note that the MR intensity and velocity images are perfectly registered since they are acquired from the same complex MR signals. More importantly, these velocity maps, through their magnitude M_v and direction θ_p distributions, constrain the possible ranges and directions of the heart boundary movement between image frames, and thus are used in constructing our segmentation criterion.

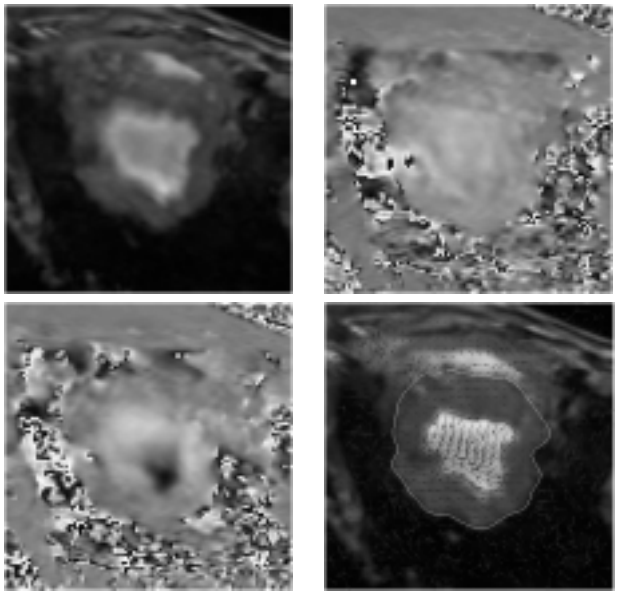

Figure 1. Canine cardiac MR phase contrast images: intensity (upper left), $x-$direction velocity (upper right), $y-$direction velocity (lower left), and plot of velocity vectors over the intensity image (lower right).

2.2. Gradient-Guided Fast Marching and Level Set Schemes for Initial Boundary Localization

The purpose of this step is to drive the propagating front to approach the myocardial boundary quickly, and the resulting contour is used for the refining step. Since the temporal sampling rate of the gated MR imaging is usually about 16 frames per cardiac cycle, the frame-to-frame movements of the boundaries are small. Hence, this step is applied to the end-diastole (ED) frame only because there is little motion artifact on the images caused by the blood flow at this stage of heart cycle. For the remaining frames, the resulting contours from the previous frames are used as the initialization contours, and only refinement step is needed.

2.2.1 Fast Marching Stage

A fast marching method is applied to the intensity image first. The front propagates from an initial location at the center of the left ventricle (LV) towards the myocardial boundaries. When searching for endocardium, the front stops at the first local gradient maximum. And when searching for epicardium, the front would pass through the first local gradient threshold, and stop at the second local gradient maximum.

Fast marching is an extremely fast scheme that only al-

lows the front moving in one direction [9]. In our implementation, the front starts to evolve from a point inside the LV on the ED frame, conforming to the evolution equation:

$$|\nabla\psi|\, F = 1 \tag{2}$$

where $|\nabla\psi|$ is represented by the gradient magnitude of the MR intensity image, F is the speed of the front. Here, $1/F$ is the parameter we use as the stopping threshold for the propagating front. Because of the nature of the ED image frame, the image gradient near the myocardial wall is quite high. After a statistical analysis of the gradient values near the boundaries, we choose an appropriate value for the thresholding parameter $1/F$, and the front would stop and form an iso-gradient contour somewhere near the true boundary.

2.2.2 Level Set Stage

Although the fast marching method provides a fast evolution scheme for front propagation, however, a global threshold alone limits the precision of the movement and stoppage of the front. Normally, the resulting contour would not reach the boundary very accurately, and further processing is needed to get closer to the boundary.

The level set method and its narrowband extension allow the front to move in both negative and positive directions [9]. A more precise boundary can be located with this scheme because of the additional consideration of the local features. For the level set evolution equation:

$$\psi_t + \hat{k_l} F| \bigtriangledown \psi| = 0 \tag{3}$$

we need to do local adjustment of $\hat{k_l}$ which is used as the stopping criteria. $\hat{k_l}$ is a gradient-dependent variable that is multiplied by the speed function F in order to cause the net speed of the front close to zero when the front approaches local gradient maximum, i.e. potential edge. However, for a typical $\hat{k_l}$ such as the one used in [4]:

$$\hat{k_l}(x,y) = \frac{1}{1 + |\bigtriangledown G_\sigma * I(x,y)|} \tag{4}$$

it is very difficult to achieve reasonable results under different imaging situations. An alternative is to use the smoothed Laplacian image, $|\nabla^2 G_\sigma * I(x,y)|$, to synthesize the speed function near boundary, and a thinning process is needed to avoid double edges [8]. Since the fast marching stage has already pushed the curve close to myocardial boundary, we can set an appropriate narrowband extension to more precisely locate the boundary within the narrowband.

The gradient and Laplacian images provide the edginess information for the stopping criterion. For epicardium, however, portion of the boundary is defined as the separation between the left and right ventricles (see the upper part of upper left image of Fig.1), and little edginess information is available. Thus, we use the average thickness of the myocardial wall between the two boundaries as a prior model constraint to help defining the epicardial boundary. If the propagating curve reaches the thickness limit, $\hat{k_l}$ will be set to zero, regardless of the edginess measure, to stop the curve.

After the level set stage, more precise boundaries are located from the gradient information alone. The left column of Figure 5 shows reasonably good segmentation results for four representing images, frames #1, #5, #9, and #13 out of sixteen frames throughout cardiac cycle. However, some problems persist. For example, in frame #13, the algorithm has difficulty to detect the true endocardial border on the right half, possibly caused by the artifacts of the heart valve. In order to alleviate these problems, we adopt a further step which utilizes additional information provided by phase velocity images to refine the curve evolution with a statistical measure of edginess within a narrowband formed around the resulting contour of the level set stage.

2.3 Gradient and Velocity Integration for Narrowband Boundary Refinement

As mentioned earlier, three elements of MR phase contrast images are integrated into a statistical edginess measure for the refinement of the boundary: the MRI intensity gradient, the phase contrast velocity magnitude M_v, and the local phase coherence of the velocity direction θ_p.

Through careful observation of the phase contrast velocity information (Fig.1), we conclude that the velocity exhibits different characteristics in terms of its magnitude and direction at different parts of the myocardium. In general, the velocity magnitude at the endocardial boundary is much smaller than that of the blood pool, and is close to zero at epicardium. As for the velocity directions, they show significant local phase coherence within the same tissue, but are chaotic at the boundaries of different tissues.

From these observations, we believe that the integration of the complementary information will provide more robust solution to the segmentation of the myocardium. In particular, during the fast contraction and fast filling periods of the cardiac cycle, the blood flow and the heart wall generate great noise artifacts on the endocardium gradient information, such as from frames #4 to #9 and from #12 to #15 of our sequence. Also, the epicardium between LV and RV is very difficult to define with intensity image alone. Phase velocity maps will provide possible remedies for the deficiency of the intensity image.

2.3.1 Local Coherence Measure of Velocity Direction

In order to derive a probability measure of the local coherence of the velocity direction, we have adopted the *Local*

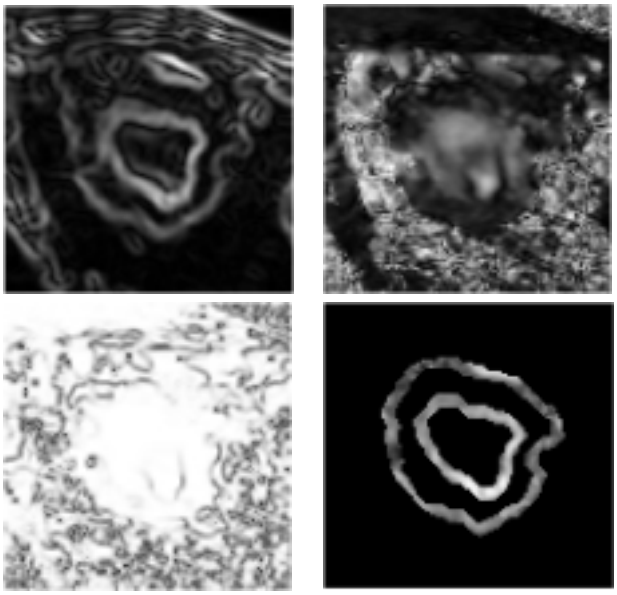

Figure 2. Contributing imaging information for integrated edginess measure: intensity image gradient (upper left), phase contrast velocity magnitude (upper right), velocity local phase coherence (lower left), and the integrated measure (lower right).

Phase Coherence (LPC) concept originally proposed for vascular structure segmentation [2]. For the velocity vector v_s at s and the velocity vector v_i of its neighbor at i, we define the $LPC(v_s)$ as:

$$f(v_s, v_i) = < v_s, v_i > /||v_s|| \; ||v_i|| \quad (5)$$

$$LPC(v_s) = \frac{1}{16}\left[\sum_{i=1}^{8} f(v_s, v_i) + 8\right] \quad (6)$$

where the summation is taken over its eight neighbors. Since $f(v_s, v_i)$ is within [-1,1], the LPC value is thus within the range of [0,1]. The smaller the LPC value, the less coherent between a point and its neighboring points, which actually means that it is more likely to be an edge point.

2.3.2 Integrated Edginess Probability Measure

In our integrated measure of edge likelihood, the optimal boundary maximizes the local gradient value, minimizes the local velocity magnitude, and minimizes the LPC value. To combine these elements together, we use a classical Bayes formulation within the narrowband (NB) of the initial contour:

$$P(b_{map}|I) = \max_{b \in NB} \frac{P(I|b)P(b)}{P(I)} \quad (7)$$

where I is the image information (intensity and phase contrast velocity), b is the myocardial boundary represented by the propagating front, b_{map} is the maximum *a posteriori* (MAP) solution, $P(b)$ is the prior probability of boundary within the narrowband, and $P(I|b)$ is the conditional probability, or likelihood, of the image given the boundary within the narrowband.

Equation (7) can be simplified by taking the natural logarithm and eliminating $P(I)$, which is the prior probability of the image data that will be equal for all points within the narrowband. Thus, it suffices to maximize:

$$M(I, b_{map}) = \max_{b \in NB} M(I, b) = \max_{b \in NB} [\ln P(b) + \ln P(I|b)] \quad (8)$$

The function M is optimized to find the MAP solution. The prior probability of the boundary $P(b)$ within the NB can be acquired from knowledge of the myocardial boundary distributions, or is assumed as uniform if no prior is available.

For a uniform prior $P(b)$ within the narrowband, the problem is further reduced to a maximum likelihood one:

$$M(I, b_{map}) = M(I, b_{ml}) = \max_{b \in NB} \ln \prod_{i=1}^{3} [\alpha_i P(I_i|b)] \quad (9)$$

where I_1 relates to the intensity image gradient I_{grad}, I_2 relates to the velocity magnitude M_v, I_3 relates to the LPC value, and α_i is normalizing weight factor for each component. In practice, the image gradient is often weighted more than the other two components, which are weighted equally.

The likelihood function $M(s)$ is calculated for every pixel s within the narrowband. A moving window $W(s)$ is constructed, centered around s inside the narrowband. The image gradient $I_{grad}(s)$ and the velocity magnitude $M_v(s)$ are normalized within window $W(s)$ by the respective local maximum values or global thresholds, whichever are larger. As explained earlier, the imaging related measures I_i are thus defined as

$$I_1(s) = I_{grad}^{normalized}(s) \quad (10)$$

$$I_2(s) = 1 - M_v^{normalized}(s) \quad (11)$$

$$I_3(s) = 1 - LPC(s) \quad (12)$$

Figure 2 shows example maps of three individual measures as well as the M value distribution of the endocardial and epicardial narrowbands formed around the initial contours.

Once the integrated edginess measure for all narrowband points are calculated, the propagating front evolves towards to the local maximum of the M map, and the resulting contour will be the most likely boundary under our criteria.

2.3.3 Contour Initialization and Multi-Scale Searching

For the first image frame, the output of the gradient-only fast marching/level set step is used as the initial boundary,

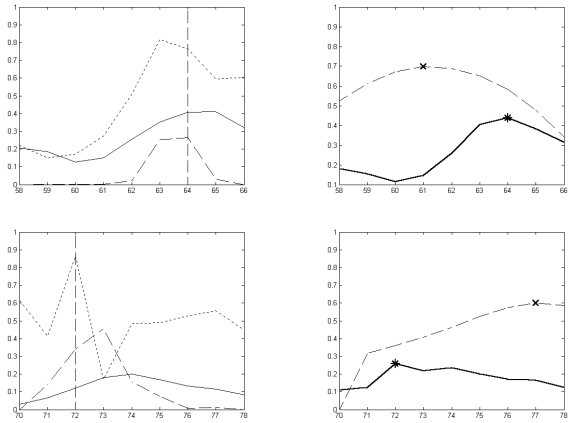

Figure 3. Edginess measures at the endocardial region (top) and epicardial region (bottom) at the right side of the left ventricle (horizontal line #54 of frame #13). Right: line profiles of I_1 (—), I_2 (...), and I_3 (- - -), where the vertical line indicates the location of the maximum integrated measure (with 5, 1, 1 weighting). Left: intensity gradient profiles used for the fast marching/level set stage (thin line, the image is smoothed a Gaussian kernel with $\sigma = 2.5$), integrated edginess measures (thick line, the image is smoothed a Gaussian kernel with $\sigma = 0.5$), where the x and $*$ indicate the respective maximum values.

and a narrowband is formed. Base on the assumption that boundaries move quite a small amount from frame to frame, for all other frames, the final resulting contours from the previous frames are used as the initialization contours:

$$\psi^n_{initial} = \psi^{n-1}_{final} \tag{13}$$

This way, not only can we save computational expense, we can also bypass some of the noises within the blood pool that may falsely stop the curve propagation at some frames.

In addition, because of the small frame-to-frame changes, only a very narrow narrowband is needed under normal situation. We also enforce thickness constraint between the endocardium and epicardium the same way as explained in section 2.2.2.

The fast marching/level set step is performed at a rather coarse scale, i.e. by using images smoothed with Gaussian kernel with large stand deviation σ. This allows us to rid of the gradient noise inside the blood region and approach true boundary. For the refinement step, however, only images smoothed with Gaussian kernels with small σ are used. This ensures us that detailed information from the images is used for the refinement of the boundary finding.

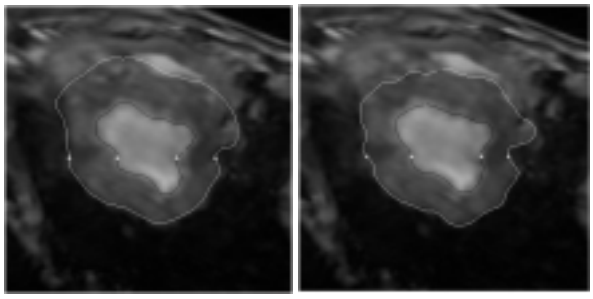

Figure 4. Segmented boundaries at frame #13 using fast marching/level set on intensity gradient information only (left), and using velocity-constrained front propagation on integrated information (right). The white dots indicate the extracted locations of the boundaries at horizontal line #54.

3 Experiment

Experiments have been conducted with cardiac MR images and the matching MR phase contrast velocities images from a normal canine study. Sixteen canine MR phase contrast velocity and magnitude images are acquired over the heart cycle. The image resolution is 1.09 mm/pixel, and the velocity intensity ranges from -150 mm/sec to 150 mm/sec, with the signs indicating the velocity directions.

Figure 3 shows the line profiles of the edginess measures, which relate to image gradient, velocity magnitude, and velocity local coherence, near the two myocardial boundary regions of the right part of the LV, on horizontal line #54 of frame #13. For endocardium, the gradient is quite strong which is evident in the similar shape between the gradient and the integrated measure curves, the influences from the two velocity measures bias the edge towards $x-$coordinate 63, instead of the other strong gradient candidates. For epicardium, the gradient is relatively weak, and the roles of the velocity measures are even more important. The two right figures also demonstrate the importance of the multi-scale search, as indicated by the drifted gradient peaks at coarse scales. Figure 4 shows the segmented boundaries at frame #13 using the fast marching/level set method on intensity gradient information only (left), and our velocity-constrained front propagation method using integrated information (right) with weighting coefficients 5, 1, 1.

The right column of Figure 5 shows the segmentation results for four representing images, frames #1, #5, #9, and #13 out of sixteen frames throughout cardiac cycle, using the integrated edginess measures. In this particular experiment, the stopping threshold for the fast marching step is 3.3×10^{-4}, since the intensity gradient is quite large for 16-

bit MR images. Because of the small changes of frame-to-frame contour locations, the narrowband size is set to ± 2 in Euclidean distance of the initial contour pixel in each case. The thickness constraint of the myocardium is 18 pixels, and uniform prior is used. And the weighting coefficients α_i are set to 5, 1, and 1 respectively. Compare to the corresponding segmentation results in Figure 5, it is easy to conclude that the velocity constrained approach has done a better job at the endocardium when the intensity information is not reliable, such as the right side of frame #13. Overall, the epicardium is more reasonably detected by the information integration approach as well.

4 Conclusion

We have presented a velocity guided front propagation framework for segmentation of myocardium from MR phase contrast image sequence. We have adopted a two-step process, using a gradient-only fast marching/level set initial estimation followed by an integrated information refinement with narrowband search. Initial results with real image sequence have been favorable.

This work is supported by HKRGC HKUST6031/01E.

References

[1] A. Chakraborty and J. S. Duncan. Game-theoretic integration for image segmentation. *IEEE PAMI*, 21(1):12–30, 1999.

[2] A. C. S. Chung, J. A. Noble, and P. Summers. Fusing speed and phase information for vascular segmentation of phase contrast mr angiograms. *Medical Image Analysis*, 6:109–128, 2002.

[3] A. J. Frangi, W. J. Niessen, and M. A. Viergever. Three-dimensional modeling for functional analysis of cardiac images: A review. *IEEE TMI*, 20(1):2–25, 2001.

[4] R. Malladi, J. A. Sethian, and B. C. Vemuri. Shape modeling with front propagation: A level set approach. *IEEE PAMI*, 17(2):158–175, 1995.

[5] F. G. Meyer, R. T. Constable, A. J. Sinusas, and J. S. Duncan. Tracking myocardial deformation using spatially constrained velocities. *IEEE TMI*, 15(4):453–465, 1996.

[6] N. Paragios. A variational approach for the segmentation of the left ventricle in mr cardiac images. *IEEE Workshop on Variational and Level Set Methods in Computer Vision*, pages 153–160, 2001.

[7] N. J. Pelc, R. J. Herfkens, A. Shimakawa, and D. Enzmann. Phase contrast cine magnetic resonance imaging. *Magnetic Resonance Quarterly*, 7(4):229–254, 1991.

[8] J. Serra. *Image Analysis and Mathematical Morphology*. Academic Press, New Yprk, 1982.

[9] J. A. Sethian. *Level Set Methods and Fast Marching Methods*. Cambridge University Press, Cambridge, 1999.

[10] S. C. Zhu and A. Yuille. Region competition: Unifying snakes, region growing, and bayes/mdl for multiband image segmentation. *IEEE PAMI*, 18(9):884–900, 1996.

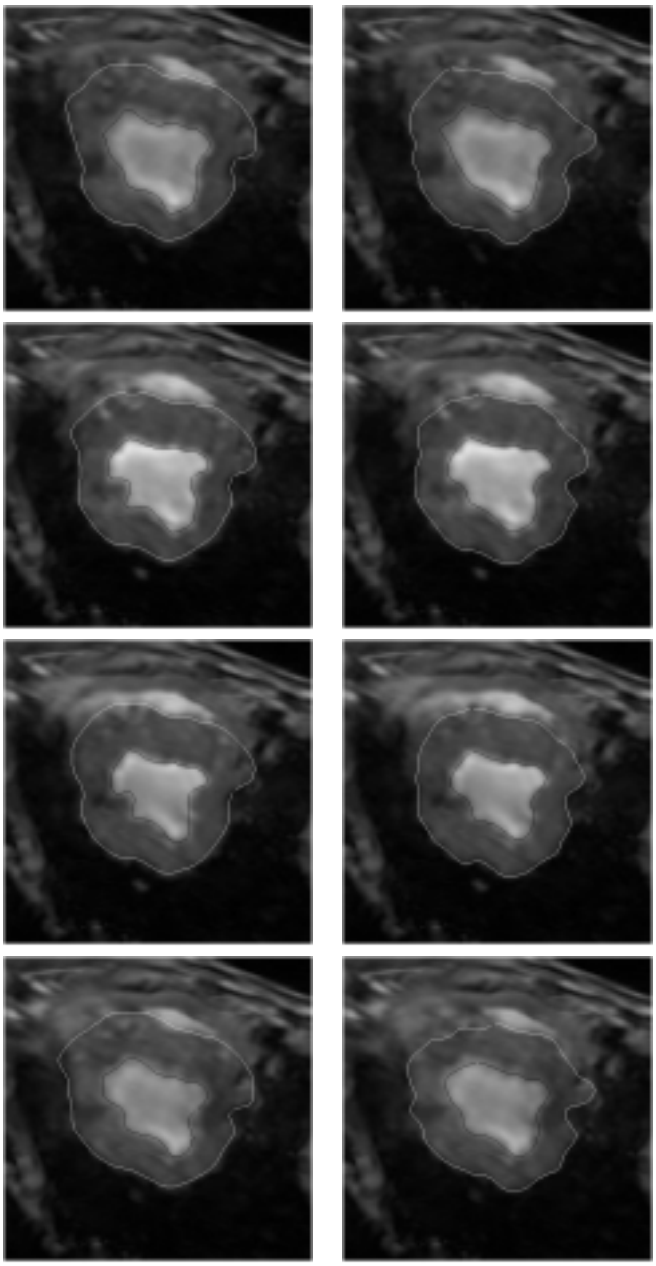

Figure 5. Segmented boundaries using intensity gradient (left) and the integrated information (right): image frames #1, #5, #9, and #13.